CREATION OF PLASMON-BASED NANOANTENNA FOR HYDROGEN PRODUCTION

[1*]Jana ROSENKRANZOVA, [1]Vasilii BURTSEV, [1]Elena MILIUTINA, [1]Vaclav SVORCIK, [1]Oleksiy LYUTAKOV

[1]University of Chemistry and Technology, Prague, Czech Republic, EU

**Corresponding author e-mail: rosenkrj@vscht.cz*

https://doi.org/10.37904/nanocon.2023.4754

Abstract

Plasmonic nanoantennas represent advanced structures that allow sub-diffraction manipulation with light energy and its simultaneous focus below the diffraction limit. Gigantic focusing of light energy in the desired targeted place allows for the realization of several phenomena, such as plasmon-induced charge energy transfer of excitation/injection of so-called hot electrons. In turn, such phenomena have found a range of applications in the fields of medicine, sensorics, photovoltaics, and chemical transformations triggering. The main obstacle to greater use of plasmon-based nanoantennas is their complex preparation route and the resulting lack of 'scalability' of the structure. In this work, we propose a simple and effective method for the preparation of plasmonic nanoantennas, in which the metal-insulator-metal (MIM) system is used. In particular, a gold grating/polystyrene/platinum heterolayer structure was created. In our design, the gold grating ensures the excitation of the surface plasmon, the polystyrene acts as a dielectric spacer between metals, and the platinum layer is responsible for the catalytic function. The created structure was subsequently used for the water splitting half reaction (hydrogen evolution - HER), which was performed in the photoelectrochemical regime. The structure was also optimized from the theoretical and experimental points of view to reach the maximum efficiency in terms of hydrogen production. After optimization of the structure parameters, we observed a doubled increase in HER efficiency under illumination with light, which corresponded to the maximum of plasmon resonance absorption bands. The proposed nanoantenna design is favoured by the simplicity of preparation and the target area of use - the production of green hydrogen with the utilization of light (potentially, sunlight) energy.

Keywords: Nanoantennas, MIM, HER, plasmon catalysis

1. INTRODUCTION

Surface plasmon resonance (SPR) [1], also known as surface plasmons [2], is the collective oscillation of valence electrons in a metal, which are in resonance with the incident light [1,2]. The resonant photon wavelengths vary for different metals [1], where the most commonly used materials are precious metals such as gold, silver and aluminium [3]. In a metal-insulator-metal (MIM) nanoantenna system [4], the interaction between light and a plasmon-active metal [5] generates surface-plasmon polaritons (SPPs) [2,4-7] at the plasmon-active metal and dielectric interface [2]. SPPs are typically observed in structures such as gratings [2,8,9] and nanowires [5]. Furthermore, photo-excited plasmonic nanostructures display a relatively high photocatalytic activity when illuminated with light of sun-like intensities. These materials are also suitable for various, not only photocatalytic, applications [1,3,10], e.g. optical devices [6,11,12], antireflection coating, nanocircuits [6], sensors [6,11-13], photovoltaics [6,7,11,13] and communication [7].

One such application is the production of green hydrogen via water splitting. This process enables the conversion of light, possibly sunlight, into chemical energy [14] for storage and later utilisation of green,

sustainable and renewable energy source [15]. When exposed to high intensity light, the MIM nanoantenna provides electrons for the hydrogen evolution reaction (HER) [1,15], as shown in equation (1).

$$2H^+ + 2e^- \rightarrow H_2 \quad (1)$$

Typically, the nanostructures used for HER are metal-semiconductor composites [1-3,13,15] or complex MIM structures [4,12,14]. In this work, we propose a simple MIM nanoantenna design made from gold as the plasmon-active metal, polystyrene (PS) as the insulator and platinum as the HER catalyst. By optimizing the nanoantenna preparation parameters, we were able to increase the efficiency of the water splitting half-reaction, using high intensity broad spectrum lamp as a light source.

2. EXPERIMENTAL PART

2.1 Materials

Standard CAT.NO.7101 microscope slides from P-Lab were used as the substrates for all samples. Solution of photoresist Su-8 was obtained from Microchem, Germany. The polystyrene (PS) was purchased from SigmaAldrich and used without further purification. Toluene (≥99.9%) was obtained from Lach-Ner, s.r.o., Neratovice, Czechia. H_2SO_4 solution (96%) was purchased from PENTA s.r.o., Prague, Czechia. Demineralized water was obtained from Sigma-Aldrich. Au target (purity 4 N) and Pt target (purity 4 N) were purchased from SAFINA a.s., Vestec, Czechia.

2.2 Sample preparation

Su-8 films were deposited on the microscope slides surface by spin-coating (1500 rpm, 30 min), dried at 80°C for 24 h and irritated by UV-source for 60 min. Pattering of Su-8 surface was accomplished using linearly polarized excimer laser beam from COMPexPro 50F KrF excimer laser (emission wavelength 248 nm, laser fluence 9 mJ·cm^{-2}, 3500 total number of pulses, beam incident angle 45°). The Au thin layers were deposited onto the patterned surface using vacuum sputtering (40 mA, 300 s, Ar atmosphere). The PS solution was deposited on the gold substrate using spin-coating (1500 rpm, 60 s) and left to dry for 8 h at room temperature in vacuum. A thin layer of Pt was deposited onto the surface using vacuum sputtering (20 mA, 110 s, Ar atmosphere), resulting in the thinnest possible conductive layer.

2.3 Measurement techniques

Several analytical techniques were used for the characterisation of the samples.

To measure the thickness of the PS layer, the Alpha-SE Ellipsometer (J. A. Wollam, USA) with CompleteEASE program was used. The thickness of the gold and platinum layers was measured using atomic peak force microscopy (AFM) (Icon (Bruker) microscope) scratch tests. The scratch tests were carried out on smooth metal films by profiling across a scratch accomplished at an angle of 90◦ relative to the surface. UV-Vis spectra was obtained using UV/VIS spectrometer Lambda 850+ (PerkinElmer, Inc., USA) with UV WinLab™ software (PerkinElmer, Inc., USA). Scanning electron microscopy (SEM) and energy-dispersive X-ray spectroscopy (EDX) (LYRA3 GMU, Tescan, CR) were collected at the operating voltage of 10 kV and a beam current of 600 pA.

Finite-difference time-domain (FTDT) simulations were performed with Comsol Multiphysics software package in 2D simulation domain, with a triangular cell (the cell size was spatially varied and was automatically determined by the software as a function of the local geometry of the structure). The parameters of Au grating (periodicity 300 nm and amplitude 80 nm) were extracted from AFM measurements. The geometry of the samples was introduced as an average of AFM measurement results. The gap size between the grating was chosen in assumption (also confirmed by SEM and AFM experiments) of their closed-packed arrangement. The PS layer was included in the experiments as a dielectric spacer between the Au grating and Pt. The

convergence of the FTDT calculation was checked by the simulation resolution increase by 50% without observable changes.

2.4 Photoelectrochemical measurements

Chronoamperometry was used for electrochemical analysis in a classic three-electrode system in a 5 ml beaker. The samples were attached as the working electrode, Ag/AgCl (sat. with 3 M KCl) electrode (BVT Technologies, CZ) as the reference electrode and a Platinum Wire electrode (BASi, USA) as the counter electrode, with 0.5 M H_2SO_4 as the electrolyte. A Palm Sens 4 potentiostat (Palm Instruments, Netherlands) controlled by PSTrace 5.8 program was used for all electrochemical measurements.

3. RESULTS AND DISCUSSION

The resulting thickness of gold was determined to be 30 nm. The thicknesses of the PS layer were 11 nm for 0.125% (PS1), 17 nm for 0.25% (PS2), 24 nm for 0.5% (PS3) and 63 nm for 1% (PS4) PS, as shown in **Figure 1**. The thickness of the Pt layer was 6 nm. **Figure 2** shows the grating of the samples with only gold (**Figure 2a**) and with Au/PS3/Pt (**Figure 2b**). As can be seen from the SEM images and EDX maps, the polymer layer 24 nm was spread uniformly and did not affect the structure of the sample. The map also indicates the presence of a homogeneous layer of platinum.

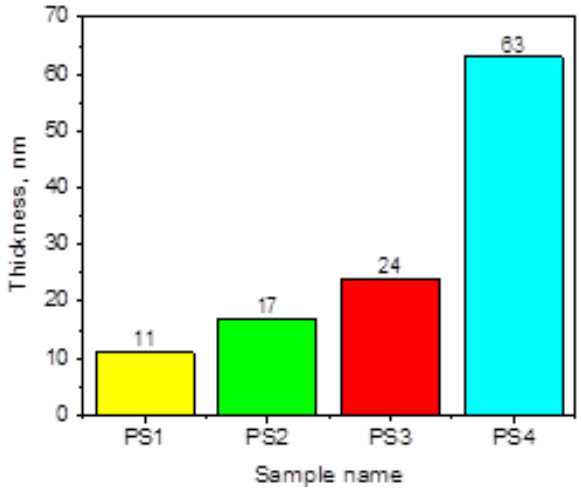

Figure 1 Thickness of PS layers for different samples preparation route

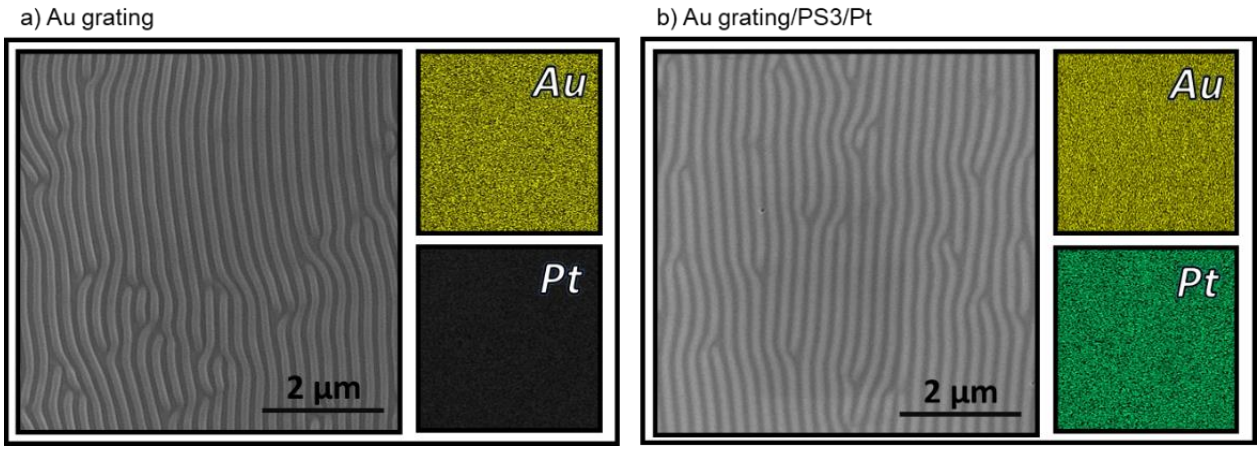

Figure 2 SEM images of grating and EDX element(s) mapping: a) grating with sputtered Au; b) grating with deposited Au, PS3 and Pt

Figure 3 shows the UV-Vis spectra of Au/PS/Pt samples, in which several absorption bands can be seen, notably at the wavelength of $\lambda \sim 600$ nm and $\lambda \sim 780$ nm, suggesting the presence of surface-plasmon polaritons (SPPs). This was further confirmed by the Finite-difference time-domain (FTDT) simulations, in which changes in the electric field upon irradiation of the samples were observed (dark red parts in **Figure 4**).

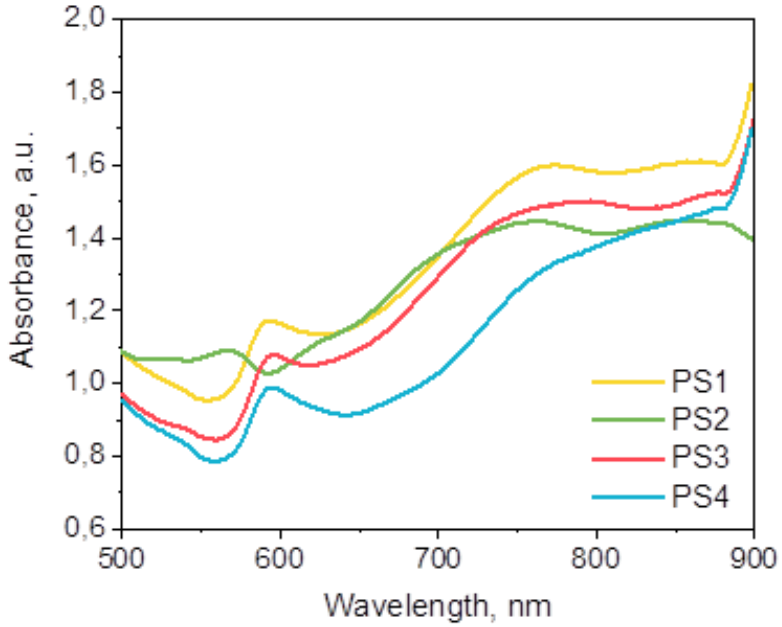

Figure 3 UV-Vis spectra of Au/PS/Pt samples

Finite-difference time-domain (FTDT) simulations the charge density distribution of **Figure 4** in turn show the distribution of electric field excited under the simulated sun illumination on nanoantenna samples (Au/PS/Pt)

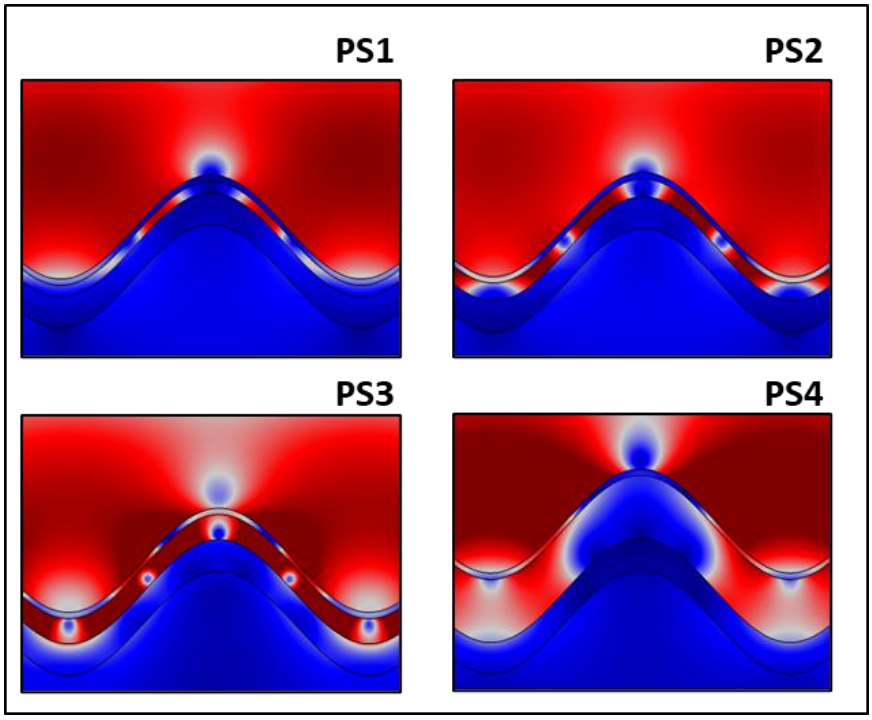

Figure 4 Finite-difference time-domain (FTDT) simulations for nanoantenna samples (Au/PS/Pt) with different PS thickness

Figure 5 shows the chronoamperometry measurements of the nanoantennas with different PS thickness. All samples display clear reaction when illuminated by broad-spectrum light source. The thickness of the polymer clearly influences the current, in which saturation occurs. Sample PS2 shows the worst results, with saturation occurring around -1.1 mA, compared to sample PS3 reaching nearly double the HER activity.

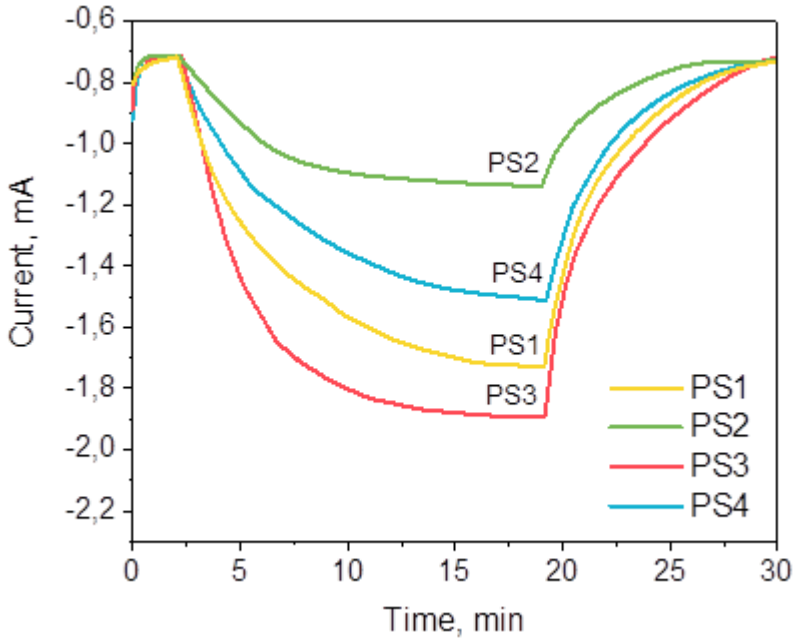

Figure 5 Chronoamperometry of Au/PS/Pt nanoantennas in the dark (beginning), exposed to light (rapid decrease in current until saturation) and without light (rapid increase in current)

4. CONCLUSION

New MIM nanoantenna preparation method was proposed using Au/PS/Pt system. This method is simpler and faster than current conventional methods and provides consistent results. Several analytical methods were used to characterize the prepared samples. Chronoamperometry was used to determine the best PS thickness for HER, from which PS3 was shown to provide the best results, reaching nearly double the current values as the worst sample.

ACKNOWLEDGEMENTS

This work was supported by the GACR under project 22-02022S

REFERENCES

[1] LINIC, S.; CHRISTOPHER, P.; INGRAM, D. B. Plasmonic-Metal Nanostructures for Efficient Conversion of Solar to Chemical Energy. *Nat. Mater.* 2011, vol. 10, no. 12, pp. 911-921. Available from: https://doi.org/10.1038/nmat3151.

[2] CHUMPOL, K. *Plasmonic Nanoantennas for Photochemistry and Photocatalysis*. Dublin, 2021. Dissertation. Trinity College Dublin.

[3] KAVANKOVA, I. Review of Nanoantennas Application. *Przegląd Elektrotechniczny.* 2023, vol. 1, no. 1, pp. 15-19. Available from: https://doi.org/10.15199/48.2023.01.03.

[4] LIU, F.; ZHANG, X.; FANG, X. Plasmonic Plano-Semi-Cylindrical Nanocavities with High-Efficiency Local-Field Confinement. *Sci. Rep.* 2017, vol. 7, no. 1, 40071. Available from: https://doi.org/10.1038/srep40071.

[5] JOHNS, P.; BEANE, G.; YU, K.; HARTLAND, G. V. Dynamics of Surface Plasmon Polaritons in Metal Nanowires. *J. Phys. Chem. C.* 2017, vol. 121, no. 10, pp. 5445-5459. Available from: https://doi.org/10.1021/acs.jpcc.6b12748.

[6] LI, N.; LAI, Y.; LAM, S. H.; BAI, H.; SHAO, L.; WANG, J. Directional Control of Light with Nanoantennas. *Adv. Opt. Mater.* 2021, vol. 9, no. 1, 2001081. Available from: https://doi.org/10.1002/adom.202001081.

[7] MARQUES LAMEIRINHAS, R. A.; TORRES, J. P. N.; BAPTISTA, A. The Influence of Structure Parameters on Nanoantennas' Optical Response. *Chemosensors.* 2020, vol. 8, no. 2. Available from: https://doi.org/10.3390/chemosensors8020042.

[8] ROSSI, S.; GAZZOLA, E.; CAPALDO, P.; BORILE, G.; ROMANATO, F. Grating-Coupled Surface Plasmon Resonance (GC-SPR) Optimization for Phase-Interrogation Biosensing in a Microfluidic Chamber. *Sensors.* 2018, vol. 18, no. 5, 1621. Available from: https://doi.org/10.3390/s18051621.

[9] ZABELINA, A.; MILIUTINA, E.; ZABELIN, D.; BURTSEV, V.; BURAVETS, V.; ELASHNIKOV, R.; NEUBERTOVA, V.; ŠŤASTNÝ, M.; POPELKOVÁ, D.; LANCOK, J.; CHERTOPALOV, S.; PAIDAR, M.; TRELIN, A.; MICHALCOVÁ, A.; ŠVORČÍK, V.; LYUTAKOV, O. Plasmon Coupling inside 2D-like TiB2 Flakes for Water Splitting Half Reactions Enhancement in Acidic and Alkaline Conditions. *Chem. Eng. J.* 2023, vol. 454, 140441. Available from: https://doi.org/10.1016/j.cej.2022.140441.

[10] BURTSEV, V.; MARCHUK, V.; KUGAEVSKIY, A.; GUSELNIKOVA, O.; ELASHNIKOV, R.; MILIUTINA, E.; POSTNIKOV, P.; SVORCIK, V.; LYUTAKOV, O. Hydrophilic/Hydrophobic Surface Modification Impact on Colloid Lithography: Schottky-like Defects, Dislocation, and Ideal Distribution. *Appl. Surf. Sci.* 2018, vol. 433, pp. 443-448. Available from: https://doi.org/10.1016/j.apsusc.2017.10.055.

[11] RYCENGA, M.; COBLEY, C. M.; ZENG, J.; LI, W.; MORAN, C. H.; ZHANG, Q.; QIN, D.; XIA, Y. Controlling the Synthesis and Assembly of Silver Nanostructures for Plasmonic Applications. *Chem. Rev.* 2011, vol. 111, no. 6, pp. 3669-3712. Available from: https://doi.org/10.1021/cr100275d.

[12] STELLING, C.; FOSSATI, S.; DOSTALEK, J.; RETSCH, M. Surface Plasmon Modes of Nanomesh-on-Mirror Nanocavities Prepared by Nanosphere Lithography. *Nanoscale.* 2018, vol. 10, no. 37, pp. 17983-17989. Available from: https://doi.org/10.1039/C8NR05499A.

[13] ZHANG, J.; ZHANG, L.; XU, W. Surface Plasmon Polaritons: Physics and Applications. *J. Phys. Appl. Phys.* 2012, vol. 45, no. 11, 113001. Available from: https://doi.org/10.1088/0022-3727/45/11/113001.

[14] GHOBADI, T. G. U.; GHOBADI, A.; SOYDAN, M. C.; VISHLAGHI, M. B.; KAYA, S.; KARADAS, F.; OZBAY, E. Strong Light-Matter Interactions in Au Plasmonic Nanoantennas Coupled with Prussian Blue Catalyst on BiVO4 for Photoelectrochemical Water Splitting. *ChemSusChem.* 2020, vol. 13, no. 10, pp. 2577-2588. Available from: https://doi.org/10.1002/cssc.202000294.

[15] SUBRAMANYAM, P.; MEENA, B.; BIJU, V.; MISAWA, H.; CHALLAPALLI, S. Emerging Materials for Plasmon-Assisted Photoelectrochemical Water Splitting. *J. Photochem. Photobiol. C: Photochem. Rev.* 2022, vol. 51, 100472. Available from: https://doi.org/10.1016/j.jphotochemrev.2021.100472.